# Development of a Simplified Model of the Hippocampal CA1 Pyramidal Neuron

Metz Júlia, Orbán-Kis K, Szilágyi T

Department of Physiology, University of Medicine and Pharmacy, Tîrgu Mureş, Romania

**Introduction:** The hippocampus is critically involved in memory formation for facts and events. Beyond its physiological role the hippocampal region is of a particular interest for scientist and clinicians as well because of its low seizure susceptibility threshold and its possible role in Alzheimer's disease and schizophrenia. The output of the hippocampus is through area CA1 pyramidal cells, thus the characterization of the pathophysiological integrative properties of its principal neurons, the pyramidal cells is of particular interest. Besides the experimental techniques in neuroscience, a large number of computational studies have been published involving CA1 pyramidal neurons.
**Aim:** The aim of our study was to develop a compartment model of CA1 pyramidal neurons that reproduces the experimentally observed main electrophysiological properties, with low computational effort.
**Material and methods:** We constructed a compartmental model of a pyramidal neuron with simplified geometry using the NEURON program. Active conductances were implemented in the soma, axon and dendrites.
**Results:** We compared our model to other computational models and found that it reproduces the main firing properties of the CA1 pyramidal neurons, with a lower computational cost.
**Conclusions:** Our model is suitable to be incorporated in a larger neural network.

**Keywords:** computational modeling, pyramidal neuron, firing pattern, active conductances

## Introduction

Neurological and mental diseases involve sometimes specific biological mechanisms localized in particular regions of the nervous system and even identifiable cellular types. Epilepsy, Alzheimer's disease and stroke heavily affect the hippocampus, which plays a key role in long term memory consolidation [1] and spatial representation [2]. Since area CA1 constitutes the hippocampal output, it is crucial to characterize the pathophysiological integrative properties of its principal neurons, the pyramidal cells. The CA1 pyramidal neuron is the most studied class of neuron in the brain and probably the better understood from both structural and functional points of view than any other type of neuron in the hippocampus.

Complementary to traditional techniques in neuroscience (*in vivo* and *in vitro* recordings), a large number of computational studies have been published involving CA1 pyramidal neurons. Until 2010 more than 50 models of CA1 pyramidal cells have been published online [3]. Twenty of these models are constructed using the NEURON simulation environment [4], and they are biophysically detailed compartmental models of pyramidal cells with active dendrites. These models investigate specific aspects of spiking pattern, synaptic scaling, dendritic excitability and integration.

Most of these model neurons are based on detailed reconstructions of real neurons and there is a large variability in their biophysical parameters. Because of the large computational cost, these model cells are not suitable for integration in a larger network.

The aim of our study was to develop a compartment model of CA1 pyramidal neuron that can reproduce the experimentally observed main electrophysiological properties, with low computational effort.

## Methods

We performed our simulations with the NEURON program (version 6.1) [4] on a Dell PC (Dual Xeon 2.4 GHz CPU, 1 GHz RAM). In order to minimize computational effort we used a simplified geometry of a CA1 hippocampal neuron, composed of 15 compartments: one for the soma, one for the axon, 4 for basal dendrites and 9 for apical dendrites.

An intracellular resistivity of $R_a$ = 150 Ωcm was used for soma and dendrites and $R_a$ = 50 Ωcm for axon. The membrane time constant was set to τm = 28 ms ($R_m$ = 28 kΩcm$^2$ and $c_m$ = 1 μF/cm$^2$). To account for spines and small dendritic branches that were not modeled explicitly, $c_m$ was increased and $R_m$ decreased by a factor of 2 in the apical dendrites (as in [9]).

To further reduce computational cost, we have chosen to limit the voltage-dependent conductances to those strictly needed to shape the action potentials (AP) (Table I). Active membrane properties included $Na^+$ [5], delayed rectifier, A-type [6], and M-type potassium conductances [7] and a non-specific $I_h$ current [7]. To take into account $Ca^{2+}$ channels opened at rest, a low-threshold $Ca^{2+}$ conductance, a $Ca^{2+}$-dependent $K^+$ conductance and a simple $Ca^{2+}$ extrusion mechanism [7] were included at uniform density and distribution in all compartments. Channel kinetics and distribution were based on the available experimental data for CA1 pyramidal neurons [8]. The individual parameters (channel density and kinetics) were initially set to those used by Shah et al. [7]. In a second step, fine tuning was performed. The simulations were run with doubled and halved values for each parameter. In this way the robustness of the model was tested and the parameter space was delimited. If the simulation gave out of range result for any of the tested electrophysiological parameters,

the parameter was returned to the original value and the parameter space boundary was marked. Several iterations were performed to map as much as possible of the parameter space. All final parameter values were within the physiological range [8].

Thus the somatic and axonal $Na^+$ conductance was higher than the dendritic one, to account for the axonal action potential initiation site, and was uniformly distributed in the apical dendrites. To account for the slow inactivation of $Na^+$ channels in the apical dendrites another gating variable was introduced in the Hodgkin-Huxley kinetic scheme [9]. The density of KA channels linearly increases with distance in the apical tree with (d/100), where d was the distance from soma in μm. Two kinds of A-type $K^+$ conductances were used, one for soma, axon, basal dendrites and apical dendrites less than 100 μm from soma, and an other for apical dendrites more than 100 μm from soma. In agreement with experimental findings on soma- and dendrite-attached patches [10], the activation curve of the distal KA conductance was shifted by -12 mV. The distribution of delayed rectifier $K^+$ conductance follows the distribution of $Na^+$ conductance. The KM conductance is constant in the soma and axon, the $Ca^{2+}$-dependent $K^+$ conductance ($I_{K\ AHP}$) has constant conductance in the soma and dendrites. The $I_h$ density increases linearly with distance in the apical tree with (3d/100), where d was the distance from soma in μm. The T-type $Ca^{2+}$ conductance is uniformly distributed in the soma and dendrites, as well as the $Ca^{2+}$ extrusion mechanism ($\tau$ = 100 ms, depth of shell is the half of the radius of the compartment).

Our model should be suitable to be incorporated in a several hundred-cell network; in this work we focused at the firing properties of the model. Our simplified pyramidal cell model had to reproduce the experimentally observed properties of action potentials (duration of approx. 1.1 ms, total amplitude of 100 mV, depolarization rate 200–400 V/s, repolarization rate 2.5–3 times slower than depolarization); the firing pattern in case of a long current injection (maximum firing frequency of approx. 100 ms, spike frequency adaptation, the amplitude of the spikes should not fall below 80% of the amplitude of the first spike) and the active back-propagation of action potentials in the dendritic tree (decrease in action potential amplitude as a function of distance from the soma and dependent on the activity of the cell).

## Results

The model didn't show spontaneous bursting activity. Single action potentials were elicited by somatic injection. The induced action potentials were characterized by the spike amplitude, depolarization and repolarization rates (measured at the 10–80% and 80–20% range of full spike amplitude from threshold), and the duration of action potential (measured at one third of full amplitude).

Model responses to long rectangular current pulses are shown in Figure 2. The amplitude of the second spike does not differ more than 10 mV from the first one.

The firing frequency decreases over time, known as spike frequency adaptation (Figure 3).

The amplitude of the action potentials decreased during the current injection. The decrease was progressive, and at the somatic level the amplitude didn't fall beyond 80% of the amplitude of the first spike (Figure 4.).

The firing frequency increased as the stimulus current was increased. The maximum firing frequency of the model neuron was 89 Hz, if higher current intensity was applied, depolarization block occurred (Figure 5).

The action potentials were actively back-propagating into the dendrites. The amplitude of the action potential was reduced with distance from the soma (Figure 6). This was due to the repolarizing action of the $K_A$ conductance. 90% reduction of the $g_{K\ A}$ (modeling the effect of 4-AP, a $K_A$ channel blocker) reduced the distance-dependent attenuation of back-propagating action potentials (Figure 6).

The amplitude of the back-propagating action potential decreased over a longer (1 sec) train of action potentials, the decrease was more evident at dendritic level (Figure 7) compared to the somatic level (Figure 4).

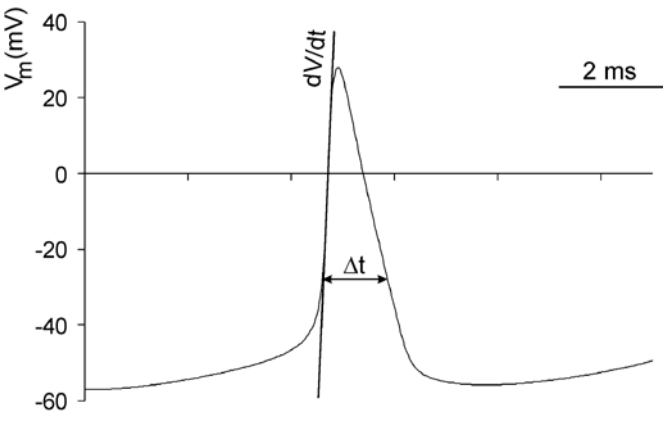


Fig. 1. Single action potential and the measurement of the depolarization rate and action potential duration (at 1/3 of full amplitude)

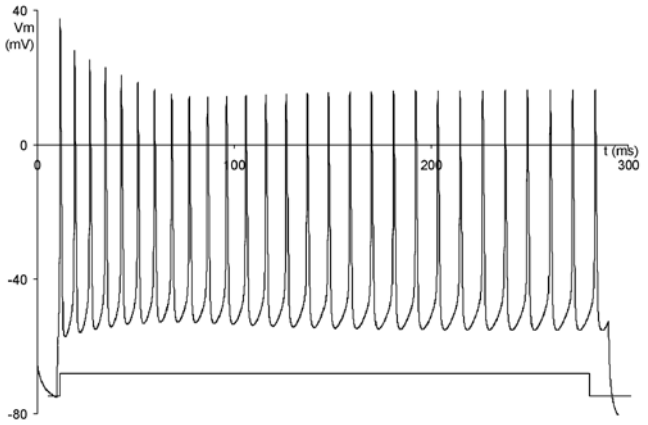


Fig. 2. The firing pattern of the simplified model cell during a 1 s long rectangular current injection (1.2nA). The amplitude of the spikes decrease with time, as well as the firing frequency.

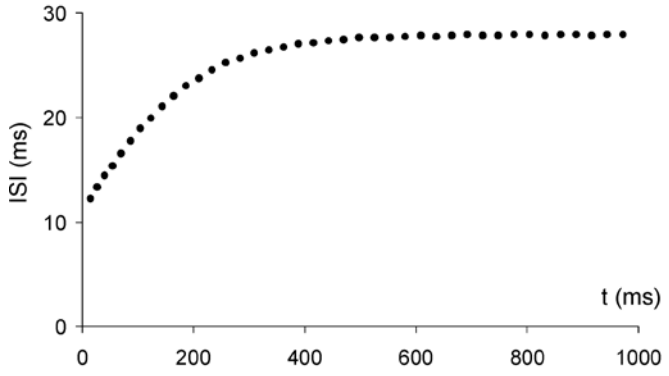


Fig. 3. Inter-spike intervals (ISI) versus the timing of the second spike during a 1 s long current injection. The initial ISI increase is faster, after several hundred msec the ISI becomes constant.

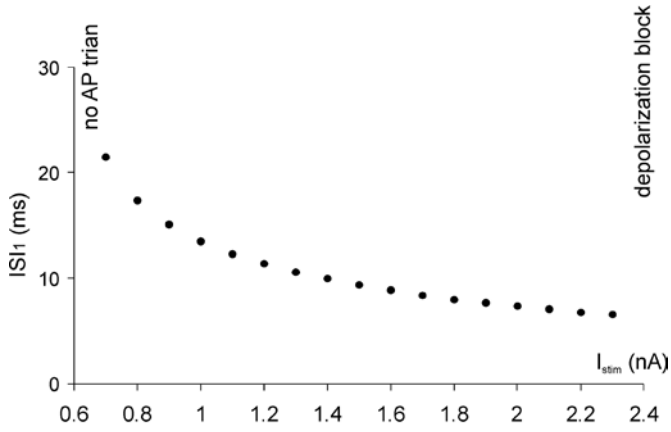


Fig. 5. The first inter-spike intervals as a function of the amplitude of current injection (1.2 nA). The firing frequency increases with the intensity of current stimulus.

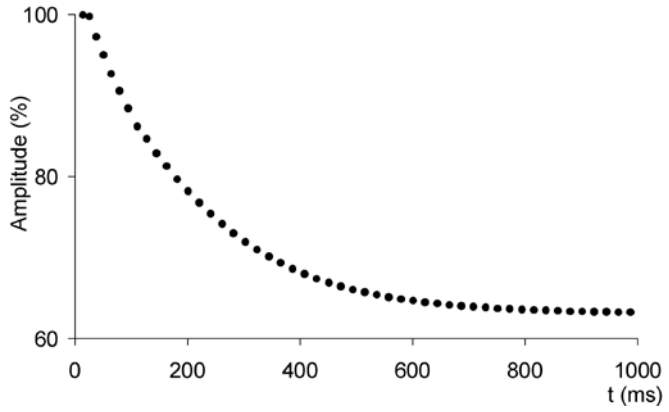


Fig. 7. The relative amplitude of the back-propagating action potentials at 505 μm from soma (distant str. radiatum) during a 1 s current injection (1.2 nA) expressed as a percent of the amplitude of the first spike.

Our simplified model could simulate 200 ms real-time data in 6.5 seconds, while the original detailed model used by Shah et al. [7] simulates the 200 ms data in 23.3 seconds, proving the computationally higher efficiency of our model.

## Discussion

Our CA1 pyramidal cell model with simplified geometry reproduced the experimentally observed properties of sin-

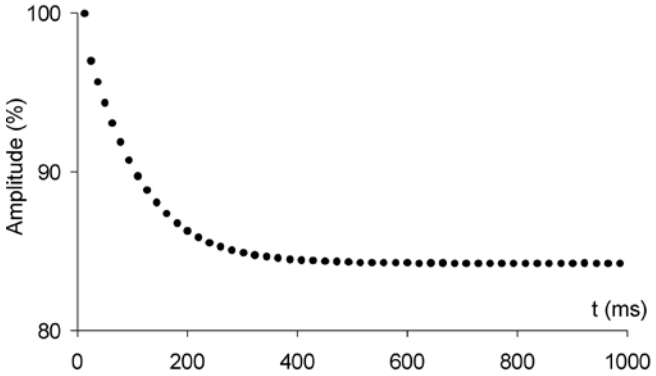


Fig. 4. The relative amplitude (compared to the amplitude of the first spike) of the action potentials at the soma during the spike train.

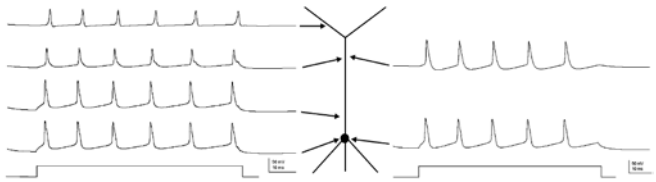

Fig. 6. Back-propagating action potentials. Left: back-propagating action potentials in the apical dendritic tree at 55 μm, 305 μm and 505 μm from soma (arrows show the recording site of the membrane potentials). Right: Back-propagating action potentials recorded at 305 μm from the soma in case of 90% reduction of gK A.

gle APs, AP train and back-propagating APs. The model contains several active ionic conductances that shape action potentials and are important in dendritic excitability.

A comparison between experimental [11,12] and model values of these action potential properties are shown in Table II. In general, values for the model are within about 20% of the average values observed experimentally.

The transient $Na^+$ current is important in the depolarizing phase of the action potential; its inactivation contributes to the spike frequency adaptation observed experimentally. The delayed rectifier $K^+$ current is important in the repolarization of the action potential. The A-type $K^+$ current is involved in the repolarization phase of the action potential, and contributes to the control of action potential firing frequency, back-propagating action potentials and temporal integration of dendritic inputs [10]. The M-type $K^+$ current is important in action potential initiation and setting the resting membrane potential. The $Ca^{2+}$-depen-dent $K^+$ current ($I_{K\ AHP}$) has major role in action potential repolarization, generation of afterhyperpolarizations, spike frequency adaptation. $I_h$ is important in setting the resting membrane potential, modifies the time course of subthreshold synaptic depolarizations [13], and has a large impact on the integration of synaptic activity. The rebound spiking mediated by $I_h$ current can have important role especially in distal dendrites, targeted by a large number of GABAergic synapses [14]. The $Ca^{2+}$ currents are important in dendritic spike generation, dendritic computation. Because of the simple geometry of the model and

**Table I. Active ionic conductances for the compartments of pyramidal cell model (S/cm²)**

| | $Na^+$ | $K_{DR}$ | $K_A$ | $K_M$ | $K_{AHP}$ | h | $Ca_T$ |
|---|---|---|---|---|---|---|---|
| Soma | 0.18 | 0.18 | 0.04 | 0.02 | $10^{-5}$ | $2.5*10^{-5}$ | $10^{-4}$ |
| Str. radiatum dendrites | 0.06 | 0.06 | 0.04–0.2 | – | $10^{-5}$ | $2.5*10^{-5}$ | $10^{-4}$ |
| Str. lacunosum-moleculare dendrites | 0.06 | 0.06 | 0.2–0.3 | – | $10^{-5}$ | $2.5*10^{-5}$ | $10^{-4}$ |
| Str. oriens dendrites | – | – | – | – | $10^{-5}$ | – | $10^{-4}$ |
| Axon | 0.36 | 0.36 | 0.04 | – | – | – | – |

**Table II. Comparison between experimental and model values of the action potential properties**

| Data source | Resting membrane potential, mV | Amplitude, mV | Duration at 1/3 of amplitude, ms | Rate of depolarization, mV/ms | Rate of repolarization, mV/ms |
|---|---|---|---|---|---|
| Experimental with sharp electrodes [19] | (-65) – (-70) | 98±8 | 1.1 | 238±16 | -85±19 |
| Experimental with patch electrodes [18] | -66.2±1.1 | 112±9 | | 381±18 | -94.8±4.7 |
| Our model | -72 | 108 | 1.2 | 340 | -73 |

**Table III. Properties of the web published CA1 pyramidal cell models**

| | Migliore 2004 | Poirazi 2003 | Shah 2008 | Royeck 2008 | Cutsuridis 2009 |
|---|---|---|---|---|---|
| No of somatic compartments | 1 | 1 | 1 | 265 | 1 |
| No of dendritic compartments | 199 | 178 | 139 | | 13 |
| No of axonal compartments | 1 | 1 | 1 | | 1 |
| Active dendrites | yes | yes | yes | yes | yes |
| Spines | yes* | no | no | no | no |
| Synapses | AMPA | AMPA<br>NMDA<br>$GABA_A$<br>$GABA_B$ | no | no | AMPA<br>NMDA<br>$GABA_A$<br>$GABA_B$ |
| $C_m$ | 1 μF/cm² * | 1 μF/cm² | 1 μF/cm² | 1 μF/cm² | 0.75 μF/cm² |
| $R_m$ | 28 kΩcm² * | non-uniform 12–200 kΩcm² | 28 kΩcm² | 70 kΩcm² | 20 kΩcm² |
| $R_a$ | 150 Ωcm, 50 Ωcm in axon | non-uniform 35–50 Ωcm | 150 Ω cm, 50 Ωcm in axon | 150 Ωcm | 150 Ωcm |
| $Na^+$ currents | $I_{Na,t}$ | $I_{Na,t}$, $I_{Na,p}$ | $I_{Na,t}$ | $I_{Na,t}$ | $I_{Na,t}$, $I_{Na,p}$ |
| $K^+$ currents | $I_{K\,DR}$, $I_{K\,A}$ | $I_{K\,DR}$, $I_{K\,A}$, $I_{K\,M}$, $I_{K\,Ca}$, $I_{K\,AHP}$ | $I_{K\,DR}$, $I_{K\,A}$, $I_{K\,M}$, $I_{K\,Ca}$, $I_{K\,AHP}$ | $I_{K\,DR}$,$I_{K\,A}$, $I_{K\,M}$, $I_{K\,AHP}$ | $I_{K\,DR}$,$I_{K\,A}$, $I_{K\,M}$, $I_{K\,Ca}$, $I_{K\,AHP}$ |
| $Ca^{2+}$ currents | – | $I_{Ca\,L}$, $I_{Ca\,T}$, $I_{Ca\,N}$, $I_{Ca\,R}$ | $I_{Ca\,L}$, $I_{Ca\,T}$, $I_{Ca\,N}$ | $I_{Ca\,L}$, $I_{Ca\,T}$, $I_{Ca\,N}$, $I_{Ca\,R}$ | $I_{Ca\,L}$, $I_{Ca\,T}$, $I_{Ca\,N}$, $I_{Ca\,R}$ |
| Other currents | $I_h$ | $I_h$ | $I_h$ | $I_h$ | $I_h$ |
| $Ca^{2+}$ accumulation/pump | no | yes | yes | yes | yes |
| Maximum firing frequency | 67 | 127 | 35 | 127 | 86 |
| Spike frequency adaptation | no | no | yes | yes | no |
| Progressive decline of back-propagating action potentials in dendrites | yes | yes | yes | no | no |

* to account for spines, in apical dendrites cm*2 and $R_m/2$ was used

the relatively small number of active conductances, our model has a significantly smaller computational cost than the web published models, therefore is more suitable for network simulations.

The back-propagation of the action potentials in the dendritic tree has important role in dendritic excitability. The amplitude of the back-propagating action potentials declines as a function of distance from the soma. Active back-propagation of dendritic action potentials is highly activity dependent; during repetitive firing, back-propagating action potentials undergo a rapid, progressive decline in amplitude [15], thus the $Ca^{2+}$ influx and the activation of dendritic $Ca^{2+}$-dependent ionic channels varies with the activity of the cell.

We compared our model to other models published on the internet. From the 20 compartmental models implemented in the NEURON simulation environment, we chose four distinct models using detailed reconstruction of CA1 pyramidal cells [5,16,17,18,7] and one with simplified geometry [19]. The detailed models were used to test different hypotheses. The model with the simplified geometry is an adaptation of one of the detailed models (Poirazi model). The geometry of the model cells and the passive and active properties of the models differ significantly from each other (Table III). We compared the action potential firing pattern of these models with our model and with experimental data.

The experimentally observed maximum firing rate (around 100 Hz) [12] was reproduced by only three models, two models had significantly lower firing rates. Our model had a firing rate similar to the experimentally observed one. The frequency adaptation of long trains of action potentials is reproduced only by two models. The back-propagation of action potentials in the apical den-

dritic tree showed a progressive decline in the action potential amplitude in three of the models. None of the tested models were able to reproduce the experimentally recorded firing pattern of the CA1 pyramidal neurons.

Although our model reproduced the firing pattern of the CA1 pyramidal cells, further testing of the model is necessary to evaluate the dendritic excitability to determine if the model responses to different excitatory and inhibitory inputs.

## Conclusions

We developed a compartmental model of a hippocampal CA1 pyramidal cell that reproduces the main features of the experimentally observed firing pattern at a low computational cost, thus the model is suitable to be incorporated in a larger (several hundred neurons) network model of the CA1 region.

## References


1. Squire, LR – Memory systems of the brain: a brief history and current perspective. Neurobiol Learn Mem 2004, 82(3): 171–7.
2. Burgess N, Maguire EA, et al. – The human hippocampus and spatial and episodic memory. Neuron 2002, 35(4): 625-41.
3. Neuron ModelDB http://senselab.med.yale.edu/modeldb/ModelList.asp?id=258 31/3/2011
4. Hines ML, Carnevale NT – The NEURON simulation environment. Neural Comput 1997, 9(6): 1179–209.
5. Migliore M, Messineo L, et al. – Dendritic Ih selectively blocks temporal summation of unsynchronized distal inputs in CA1 pyramidal neurons. J Comput Neurosci 2004, 16(1): 5–13.
6. Migliore M, Hoffman DA, et al. – Role of an A-type K+ conductance in the back-propagation of action potentials in the dendrites of hippocampal pyramidal neurons. J Comput Neurosci 1999, 7(1): 5–15.
7. Shah MM, Migliore M, et al. – Functional significance of axonal Kv7 channels in hippocampal pyramidal neurons. Proc Natl Acad Sci U S A 2008, 105(22): 7869–74.
8. Migliore M, Shepherd GM – Emerging rules for the distributions of active dendritic conductances. Nat Rev Neurosci 2002, 3(5): 362–70.
9. Migliore M – Modeling the attenuation and failure of action potentials in the dendrites of hippocampal neurons. Biophys J 1996, 71(5): 2394–403.
10. Hoffman DA, Magee JC, et al. – K+ channel regulation of signal propagation in dendrites of hippocampal pyramidal neurons. Nature 1997, 387(6636): 869–75.
11. Staff NP, Jung HY, et al. – Resting and active properties of pyramidal neurons in subiculum and CA1 of rat hippocampus. J Neurophysiol 2000, 84(5): 2398–408.
12. Storm JF – Action potential repolarization and a fast after-hyperpolarization in rat hippocampal pyramidal cells. J Physiol 1987, 385: 733–59.
13. Buhl EH, Halasy K, et al. – Diverse sources of hippocampal unitary inhibitory postsynaptic potentials and the number of synaptic release sites. Nature 1994, 368(6474): 823–8.
14. Ascoli GA, Gasparini S, et al. – Local control of postinhibitory rebound spiking in CA1 pyramidal neuron dendrites. J Neurosci 2010, 30(18): 6434–42.
15. Spruston N, Schiller Y, et al. – Activity-dependent action potential invasion and calcium influx into hippocampal CA1 dendrites. Science 1995, 268(5208): 297–300.
16. Poirazi P, Brannon T, et al. – Arithmetic of subthreshold synaptic summation in a model CA1 pyramidal cell. Neuron 2003, 37(6): 977–87.
17. Poirazi P, Brannon T, et al. – Pyramidal neuron as two-layer neural network. Neuron 2003, 37(6): 989–99.
18. Royeck M, Horstmann MT, et al. – Role of axonal NaV1.6 sodium channels in action potential initiation of CA1 pyramidal neurons. J Neurophysiol 2008, 100(4): 2361–80.
19. Cutsuridis V, Cobb S, et al.–- Encoding and retrieval in a model of the hippocampal CA1 microcircuit. Hippocampus 2009, 20(3): 423–46.